Rational Design of Stable Functional Metal–Organic Frameworks

Zhijie Chen,[1,2,*] Kent O. Kirlikovali,[3] Le Shi,[1,2] and Omar K. Farha[3,4,*]

[1] Stoddart Institute of Molecular Science, Department of Chemistry, Zhejiang University, Hangzhou 310058, P. R. China

[2] Zhejiang-Israel Joint Laboratory of Self-Assembling Functional Materials, ZJU-Hangzhou Global Scientific and Technological Innovation Center, Zhejiang University, Hangzhou 311215, China

[3] Department of Chemistry and International Institute for Nanotechnology, Northwestern University, 2145 Sheridan Road, Evanston, Illinois 60208, United States

[4] Department of Chemical & Biological Engineering, Northwestern University, Evanston, Illinois 60208, United States

*Corresponding author. Email: zhijiechen@zju.edu.cn, o-farha@northwestern.edu

MAIN TEXT

ABSTRACT: Functional porous metal–organic frameworks (MOFs) have been explored for a number of potential applications in catalysis, chemical sensing, water capture, gas storage, and separation. MOFs are among the most promising candidates to address challenges facing our society related to energy and environment, but the successful implementation of functional porous MOF materials are contingent on their stability; therefore, the rational design of stable MOFs plays an important role towards the development of functional porous MOFs. In this Focus article, we summarize progress in the rational design and synthesis of stable MOFs with controllable pores and functionalities. The implementation of reticular chemistry allows for the rational top-down design of stable porous MOFs with targeted topological networks and pore structures from the pre-selected building blocks. We highlight the reticular synthesis and applications of stable MOFs: 1) MOFs based on high valent metal ions (e.g., Al^{3+}, Cr^{3+}, Fe^{3+}, Ti^{4+} and Zr^{4+}) and carboxylate ligands; 2) MOFs based on low valent metal ions (e.g., Ni^{2+}, Cu^{2+}, and Zn^{2+}) and azolate linkers. We envision that the synthetic strategies, including modulated synthesis and post-synthetic modification, can potentially be extended to other more complex systems like metal-phosphonate framework materials.

Introduction

Metal–organic frameworks (MOFs), assembled from metal-containing nodes and organic linkers via coordination bonds, are a class of nanoporous crystalline materials.[1-5] The versatile choice of inorganic and organic building units, along with the periodic nature of framework structures, permits for the targeted synthesis of MOFs with tunable pore apertures, pore sizes, and surface areas. In particular, reticular chemistry, which is a powerful strategy for constructing extended framework structures in a controlled fashion, provides a rational approach for the top-down design and precise spatial arrangement of MOFs from simple inorganic and organic building

components at the molecular level.[6-14] Generally, researchers will first design a "blueprint" for a target structure by encoding the molecular geometry and accurate arrangement of building units.[7, 15] Then, they will select a practical synthetic strategy, guided by the "blueprint", for making the crystalline, large, and extended structures with high precision by considering the interactions, directionality, and geometric information of molecular building units.

Such deliberate design and synthesis process based on reticular chemistry offer a route to generate MOFs with excellent control over porous framework structures, and as a result, related programmable functionalities. Researchers have explored the use of functional nanoporous MOFs that feature ultrahigh surface areas and porosities and consist of precisely tailorable pore geometry and structures to meet global challenges associated with both energy-based applications and the environment,[16, 17] including heterogeneous catalysis,[5, 18-20] water adsorption,[17, 21, 22] toxic chemical removal,[23-27] and gas storage and separation,[28-31] among others. In this regard, accessing a wide variety of MOFs with high stability is of great importance.

In recent years, MOF chemists have studied many important factors that contribute to MOF stability,[2, 32, 33] such as exploring how the strength of the metal–ligand coordination bonds, the hydrophobicity of the pore surface, and the operating conditions affect the stability of the framework. Generally, MOF stability follows Pearson's hard/soft acid/base (HSAB) principle (**Fig. 1**).[2, 32, 34, 35] For instance, stable MOFs are often based on the assembly of hard high valent metal ions (e.g., Al^{3+}, Cr^{3+}, Fe^{3+}, Ti^{4+} and Zr^{4+}) and hard carboxylate ligands, or soft low valent metal ions (e.g., Ni^{2+}, Cu^{2+}, and Zn^{2+}) and soft azolate linkers.[2, 32-34, 36, 37] MOFs formed from these combinations have remarkable thermodynamic stability due to the strong metal–ligand coordination bonds. The kinetic stability of these MOFs, on the other hand, can be further tuned by adjusting the rigidity and length of linkers, connectivity of inorganic nodes, and hydrophobicity

of the surface or interfaces.[32, 38] To this end, the rational design of stable MOFs, aided by the reticular chemistry, is crucial for the precise installation of functionalities and the ultimate implementation of MOFs in targeted applications.

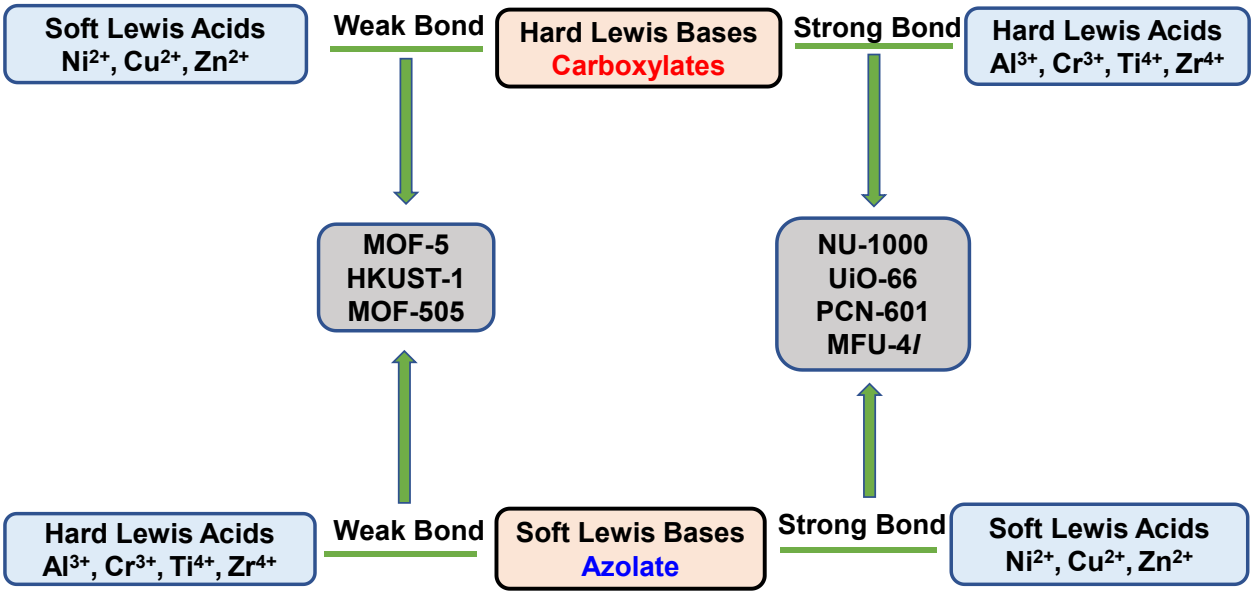

Fig. 1 Illustration of rational synthesis strategies for stable MOFs, which often agrees with Pearson's hard/soft acid/base (HSAB) principle.

In this Focus Article, we will provide an overview of some representative examples regarding the rational synthesis of stable MOFs with controllable structures and functionalities. We will summarize the blueprint network strategy for designing and synthesizing stable porous MOFs via reticular chemistry, including MOFs based on high valent metal ions (e.g., Al^{3+}, Cr^{3+}, Fe^{3+}, Ti^{4+} and Zr^{4+}) and carboxylate ligands, as well as MOFs based on low valent metal ions (e.g., Ni^{2+}, Cu^{2+}, and Zn^{2+}) and azolate linkers (**Fig. 2**). In addition, we will also review practical synthetic tools, such as modulated synthesis and post-synthetic modification, that enable the precise exploration of structure–property relationships. We will then conclude by offering our perspective on how the rational design of stable porous MOFs will shape the future of this field.

This Focus Article aims to provide readers both a fundamental understanding of design strategies that afford stable MOFs and how these types of porous materials can be employed in a diverse range of applications.

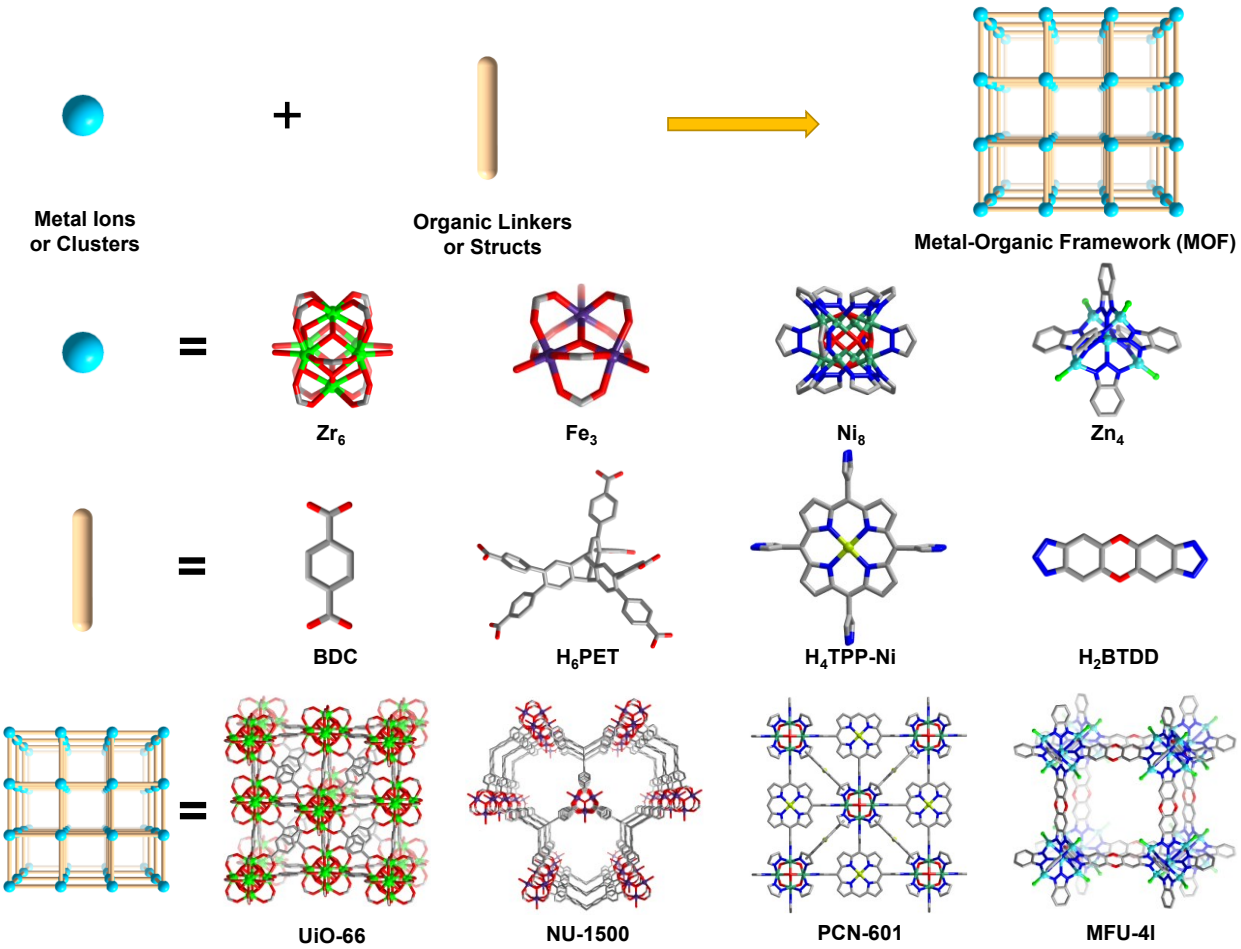

Fig. 2 Schematic representation of stable MOFs and their building units.

Reticular chemistry for stable MOFs

Reticular chemistry has been extensively applied to the rational synthesis of MOFs, such as Zn-carboxylate MOFs[39] and Cu-carboxylate MOFs[40], and plays a prominent role in the development of functional porous MOFs. In recent years, reticular chemistry has grown into a vital tool that enables access to stable MOFs, including Zr-carboxylate MOFs, Fe/Cr/Al-carboxylate

MOFs, Zn-triazolate MOFs, Ni-pyrazolate MOFs.[15, 33, 41, 42] Employing reticular chemistry as a tool for MOF synthesis comprises three complementary approaches. First, researchers can use a targeted net, which is often an edge-transitive net (i.e., a net with one type of edge) or a related minimal edge-transitive net, to guide the synthesis of MOFs from preselected inorganic and organic building units. Second, researchers can apply isoreticular chemistry, including isoreticular functionalization, expansions, and contractions, to functionalize or fine-tune the pore structures of MOFs. Third, researchers can use reticular chemistry to employ serendipitous exploration approaches that may afford the discovery of unexpected MOF structures. During these processes, unambiguous structural determination is crucial to understand the MOF structure and the related intrinsic properties, and in particular, single-crystal X-ray diffraction (SCXRD) analysis often plays a significant role in unveiling the MOF structure with atomic-level precision. In this regard, growing nearly perfect single crystals of stable MOFs that are suitable sizes for SCXRD analysis can present an obstacle for researchers in this field. In some cases, researchers have overcome these challenges by employing high-resolution transmission electron microscopy (HR-TEM) to reveal the structures of MOFs with small particle sizes that are unsuitable for SCXRD analysis.[43, 44]

In 2019, we systematically summarized the progress of rationally synthesizing Zr-carboxylate MOFs via reticular chemistry.[41] In general, high-valent metal-containing carboxylate-based MOFs and low-valent metal-containing azolate-based MOFs demonstrate high thermodynamic stability due to the strong metal–ligand coordination bonds in these MOFs, which is in agreement with the HSAB principle. However, strong metal–ligand coordination bonds often give rise to MOF particles with poor crystallinity and small crystal sizes, which increases the difficulty in unambiguously determining the MOF structure. As a result, researchers developed an

approach to increase the size of MOF crystallites by regulating the ratio of benzoic acid (modulator) to zirconium salts, which affords Zr-carboxylate MOFs with large crystallite sizes.[45]

The synthesis and applications of stable porous MOFs

Metal-carboxylate MOFs

In this section, we will elaborate on the rational synthesis and applications of stable MOFs assembled from carboxylate ligands and high valent metal ions, including Al^{3+}, Cr^{3+}, Fe^{3+}, Ti^{4+} and Zr^{4+}. Trinuclear clusters comprised of trivalent metal (e.g., Al^{3+}, Cr^{3+}, and Fe^{3+}) are common building blocks used to synthesize metal-carboxylate MOFs, where the 6-connected metal nodes can geometrically be viewed as trigonal prisms. MOF-235[46] and MIL-88[47], which form the edge-transitive **acs** net, represent two early examples of MOFs based on trigonal prismatic trinuclear metal clusters and ditopic organic linkers. Researchers observed a reversible flexible behavior in a series of isoreticular MIL-88 MOFs based on chromium or iron trinuclear building blocks, with fumarate, terephthalate, 2,6-naphthalenedicarboxylate, and 4,4'-biphenyldicarboxylate linkers used in MIL-88A, -B, -C, and -D, respectively. MIL-101(Cr) and MIL-100(Cr), which feature the **mtn** net, are well-studied stable mesoporous MOFs based on chromium trinuclear building units and carboxylate-based terephthalate and trimesate ligands, respectively. Due to their significant stability and high porosity, MIL-101(Cr) and MIL-100(Cr) have been studied as efficient catalysts for oxidation reactions[48, 49] and adsorption-based gas separation applications.[50] The synthesis of Cr-MOFs, including MIL-101(Cr) and MIL-100(Cr), often involves the use of hydrofluoric acid, which is highly corrosive and toxic. Also, single crystals of these Cr-MOFs are typically difficult to obtain, which could be due to the fact that the chromium–carboxylate coordination bonds are kinetically inert. The Zhou group overcame this challenge by employing a post-synthetic strategy

to synthesize a stable Cr-MOF in single crystal form, denoted as PCN-426-Cr(III), that involved a metal exchange of PCN-426-Mg with Cr(II) salts and then oxidization to Cr(III) in air.[51] The Zhou group further synthesized a mesoporous Cr-MOF, PCN-333-Cr(III) – an extended version of MIL-100(Cr) with the **mtn** topology, via the reduction of Fe^{3+} in PCN-333-Fe(III) by Cr^{2+}.[52] They then explored the robust and stable PCN-333-Cr as a platform to incorporate alkylamines for carbon dioxide (CO_2) capture and found that alkylamine-functionalized MOF displayed a significant CO_2 adsorption capacity at room temperature.

The combination of metal trinuclear clusters and tetracarboxylate ligands affords MOFs based on the 4,6-connected **soc** net. Eddaoudi and coworkers synthesized the first **soc**-MOF assembled from 6-connected indium trinuclear building blocks and 4-connected 3,3',5,5'-azobenzenetetracarboxylate ligands.[53] This **soc**-MOF platform can further be extended to even more stable MOFs based on iron or aluminum trinuclear building blocks.[54, 55] Moreover, researchers demonstrated that **soc**-MOF, which also refers to MIL-127 and PCN-250, can be used for a set of applications ranging from catalysis and toxic gas capture to gas separation and storage.[56-59 60] Remarkably, the rational selection of organic ligands with appropriate geometrical information results in the isoreticular expansion of prototype **soc**-MOFs. For instance, the isoreticularly expanded Al-**soc**-MOF-1, which is assembled from oxo-centered trinuclear aluminum building blocks and quadrangular ligands, displays exceptionally high microporosity with an apparent Brunauer-Emmett-Teller (BET) surface area of 5585 $m^2\ g^{-1}$ and an experimental pore volume of 2.3 $cm^3\ g^{-1}$.[61] This elegantly designed stable MOF realizes the best compromise between gravimetric and volumetric gas capacities towards the storage of hydrogen, oxygen, and carbon dioxide. The chromium-based analogue, denoted as Cr-**soc**-MOF-1 and synthesized from

the post-synthetic metal exchange of Fe-**soc**-MOF-1, is hydrolytically stable and displays an excellent reversible water vapor uptake of 1.95 g g^{-1} at the relative humidity of 70%.[22]

Combining metal trinuclear clusters and robust trigonal prismatic organic ligands should form MOFs based on the 6-connected **acs** net, such as NU-1500. Notably, the NU-1500 series is made from iron or chromium trinuclear building units and trigonal prismatic triptycene-based organic ligands to afford robust and rigid MOFs, which contrasts the flexible MIL-88 series that is comprised of the same trinuclear building unit.[62] Similar to the previously reported PCN-426-Cr, PCN-333-Cr, and Cr-**soc**-MOF-1, NU-1500-Cr was obtained from NU-1500-Fe via post-synthetic transmetalation. NU-1500-Cr is hydrolytically stable and highly porous, with an apparent BET surface area of 3580 m^2 g^{-1} and an experimental pore volume of 1.24 cm^3 g^{-1}. The nitrogen adsorption isotherms at 77 K of NU-1500-Cr activated directly from water and acetone are almost undistinguishable, suggesting its high hydrolytic stability. Moreover, NU-1500-Cr displays a high water capacity of about 1.09 g g^{-1} at P/P_0 = 0.90 and 298 K, and it can maintain this uptake after multiple adsorption-desorption cycles. The extended version of NU-1500, NU-1501, displays an apparent BET surface area of 7310 m^2 g^{-1} (when fulfilling all four BET consistency criteria) and an experimental pore volume of 2.91 cm^3 g^{-1},[16] which places the highly porous NU-1501 among the best adsorbents for both hydrogen and methane storage.

Titanium-based MOFs comprise an attractive class of stable MOFs due to their potential optoelectronic and photocatalytic applications.[63] However, reported structures of Ti-MOFs are still rare because of synthetic challenges associated with these materials.[64] For example, Ti^{4+} salts are often very reactive and can easily hydrolyze under ambient conditions, which results in the formation of amorphous products during MOF synthesis. In this section, we selectively highlight a few examples that illustrate both the rational synthesis and unique applications of Ti-MOFs (**Fig.**

3). MIL-125 is the first crystalline and porous titanium-carboxylate MOF, and it is assembled from octanuclear titanium clusters and dicarboxylate ligands under mixed solvent conditions of *N,N*-dimethylformamide and methanol.[65] An isoreticular amine-functionalized MOF, NH_2-MIL-125, was found to be a competent catalyst for the photocatalytic reduction of carbon dioxide under visible light irradiation.[66] COK-69 is a flexible Ti-MOF with the **acs** net that is assembled from the combination of trans-1,4-cyclo-hexanedicarboxylate ligands and relatively uncommon trinuclear titanium building blocks.[67] Under inert conditions, the blue-gray COK-69-Ti(III) can be isolated, and it can then easily transform into the off-white COK-69-Ti(IV) upon exposure to air. In another example, the combination of porphyrinic ligands and hexanuclear titanium-based cluster precursors results in the synthesis of an unprecedented porphyrinic Ti-MOF (PCN-22) based on the Ti_7O_6 oxo-cluster,[68] which can be used for the photocatalytic oxidation of benzoic alcohol. Notably, the Zhou group developed a promising synthetic approach, denoted as high valence metathesis and oxidation, for the synthesis of a series of Ti-MOFs. For example, MIL-100(Sc), PCN-333(Sc), MOF-74(Zn), and MOF-74(Mg) were first subjected to post-synthetic metal exchanged conditions with Ti(III), followed by a mild and facile metal node oxidation step in air.[69] These resulting Ti-MOFs can be used for the photodegradation of methylene blue.

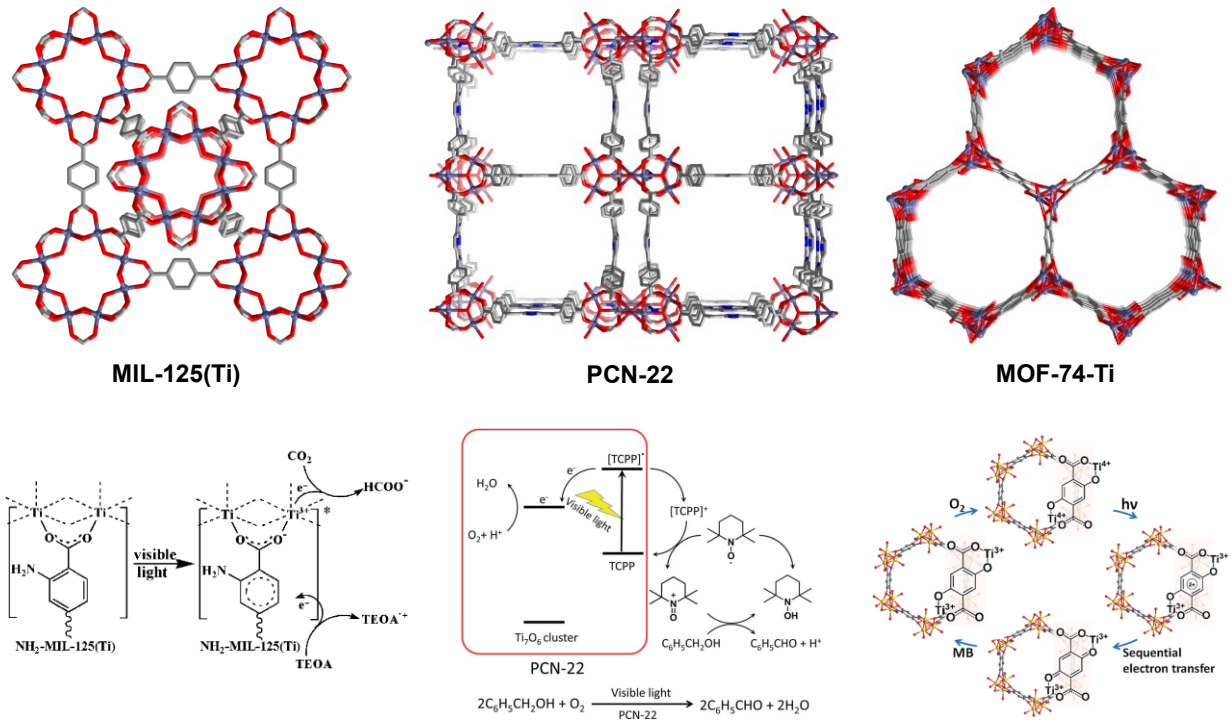

Fig. 3 Illustration of structures and relevant applications of stable Ti-MOFs. The structures of MIL-125-Ti, PCN-22 and MOF-74-Ti, and its photo catalysis properties. Figure of carbon dioxide reduction reprinted with permission from ref[66], Copyright 2012 John Wiley and Sons; figure of benzyl alcohol oxidation reaction reprinted from ref[68] with permission from the Royal Society of Chemistry, Copyright 2015; figure of photodegradation reproduced from ref[69] with permission from the Royal Society of Chemistry, Copyright 2016.

Zr-MOFs comprise an outstanding subclass of stable MOFs that paved the way for the rational synthesis of functional MOFs.[3, 41, 70] Here, we will select a few examples from our group to illustrate the role of reticular chemistry in the rational synthesis of this class of MOFs. For instance, our group recently explored the synthesis of Zr-MOFs with ligands based on a unique [2.2]paracyclophane (PCP) scaffold.[71] The assembly of Zr_6 nodes and ditopic carboxylate ligands results in the synthesis of two Zr-MOFs: the 2-dimensional NU-700 and NU-405, which is based on the 12-connected **fcu** net. Due to the out-of-plane nature of the PCP building blocks, two types

of 4-connected tetracarboxylate ligands can be obtained by organic synthesis. The combination of tetracarboxylate ligands and Zr_6 nodes leads to the formation of a series of robust Zr-MOFs, includingf NU-1800 with the 4,8-connected **flu** net, NU-602 with the 4,6-connected **she** net, and NU-913 with the 4,8-connected **scu** net (**Fig. 4**). These MOFs have been explored for water sorption experiments. The hydrolytic stability of NU-913 can further be enhanced by tuning the coordination environment of Zr_6 nodes with the hydrophobic trifluoroacetic acid (TFA) instead of acetic acid. The hydrolytically stable NU-913-TFA displays a high water capacity with reversible uptake. In addition, our group also synthesized the Zr-MOF NU-1107, which features the 4,12-connected **ftw** net and is based on tetracarboxylate ligands with the cyclen core.[72] The flexible cyclen cores in NU-1107 can serve as efficient chelating groups for a set of transition-metal ions (e.g., Co, Cu, Pd, and Ag). These metal-docked isostructural Zr-MOFs were explored for use in the separation of xenon and krypton mixtures, and NU-1107-Ag(I), which exhibits the strongest framework polarizability, shows the best performance separating xenon and krypton mixtures.

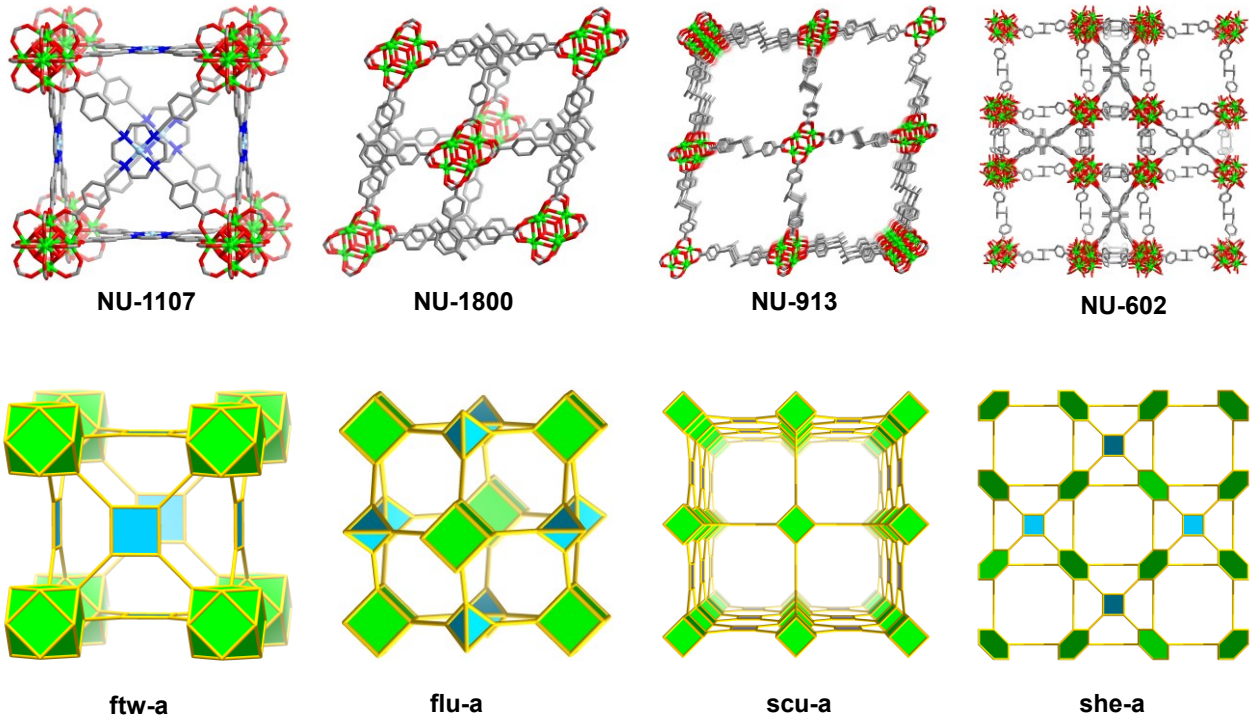

Fig. 4 Structures of a series of Zr-MOFs (top) and their topological nets (down).

In another work, our group developed a *de novo* linker installation strategy to synthesize a series of stable and robust Zr-MOFs based on the NU-600 platform with the 4,6-connected **she** net (**Fig. 5**). The pristine NU-600 is made from 6-connected Zr_6 nodes and 4-connected 1,4-dibromo-2,3,5,6-tetrakis(4-carboxyphenyl)benzene (H_4TCPB-Br_2) ligands.[73] NU-600 features two types of free coordination sites with node-to-node distances of 6.5 Å and 11.1 Å, respectively. These pockets are suitable for accommodating ditopic organic linkers, including 1,4-dicarboxybenzene (H_2BDC) and biphenyl-4,4′-dicarboxylic acid (H_2BPDC) with lengths of ~ 6.8 Å and ~ 11.3 Å, respectively. The resulting multicomponent MOFs, denoted as NU-603 with BDC incorporated, NU-604 with BPDC incorporated, and NU-605 with both BDC and BPDC incorporated, show enhanced hydrolytic stability and water sorption performance compared to the prototype NU-600. In particular, NU-604 and NU-605 maintain their high water uptakes after multiple cycles of water adsorption–desorption experiments, which can likely be attributed to the higher Zr_6 node connectivity in these MOFs relative to that of the pristine NU-600.

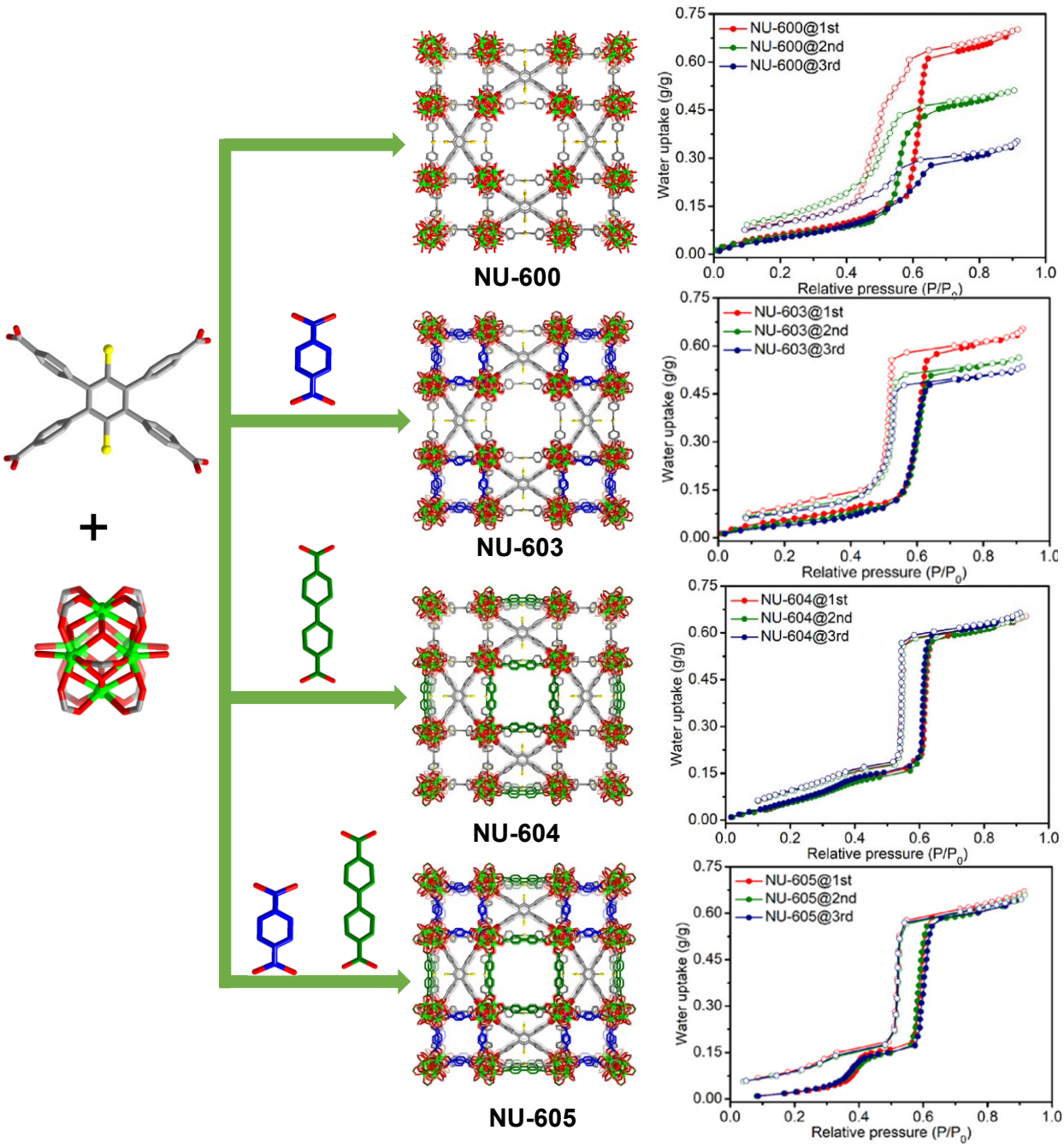

Fig. 5 Rational synthesis of multivariate MOFs based on the prototype NU-600 and their water adsorption−desorption isotherms at 298 K. Reproduced from ref[73] with permission from the American Chemical Society (Copyright 2023)

Metal-azolate MOFs

Next, we will discuss the synthesis and applications of MOFs from the assembly of soft, low-valent metal ions and soft azolate linkers, particularly the metal-pyrazolate and metal-triazolate MOFs. Metal-azolate frameworks are a class of well-studied MOFs that feature a particularly high degree of base stability, which renders them promising for use in applications under alkaline conditions.[33, 36] Due to the limited length of this article, we will not include zeolitic imidazolate frameworks, which are another well-known class of stable azolate-based MOFs.[74, 75] In one example, the combination of 12-connected Ni_8 clusters and linear ditopic bipyrazole ligands leads to the synthesis of Ni-MOFs with the 12-connected **fcu** net (**Fig. 6**).[42, 76] Galli, Bordiga, and co-workers reported an early example of Ni-pyrazolate MOFs from the assembly of octanuclear nickel-based clusters and pyrazolate ligands (i.e., 4,4′-bis(1H-pyrazol-4-yl)biphenyl and 2,6-bis(1H-pyrazol-4-yl)pyrrolo[3,4-f]isoindole-1,3,5,7(2H,6H)-tetrone).[76] In another study, Navarro, Barea, and co-workers designed and synthesized an isoreticular series of porous azolate-based MOFs by assembling the Ni_8 nodes and ditopic azolate linkers.[42] These hydrophobic Ni-MOFs can be used to capture the harmful volatile organic compound diethylsulphide – a simulant of the chemical warfare agent mustard vesicant gas – under moisture-rich conditions.

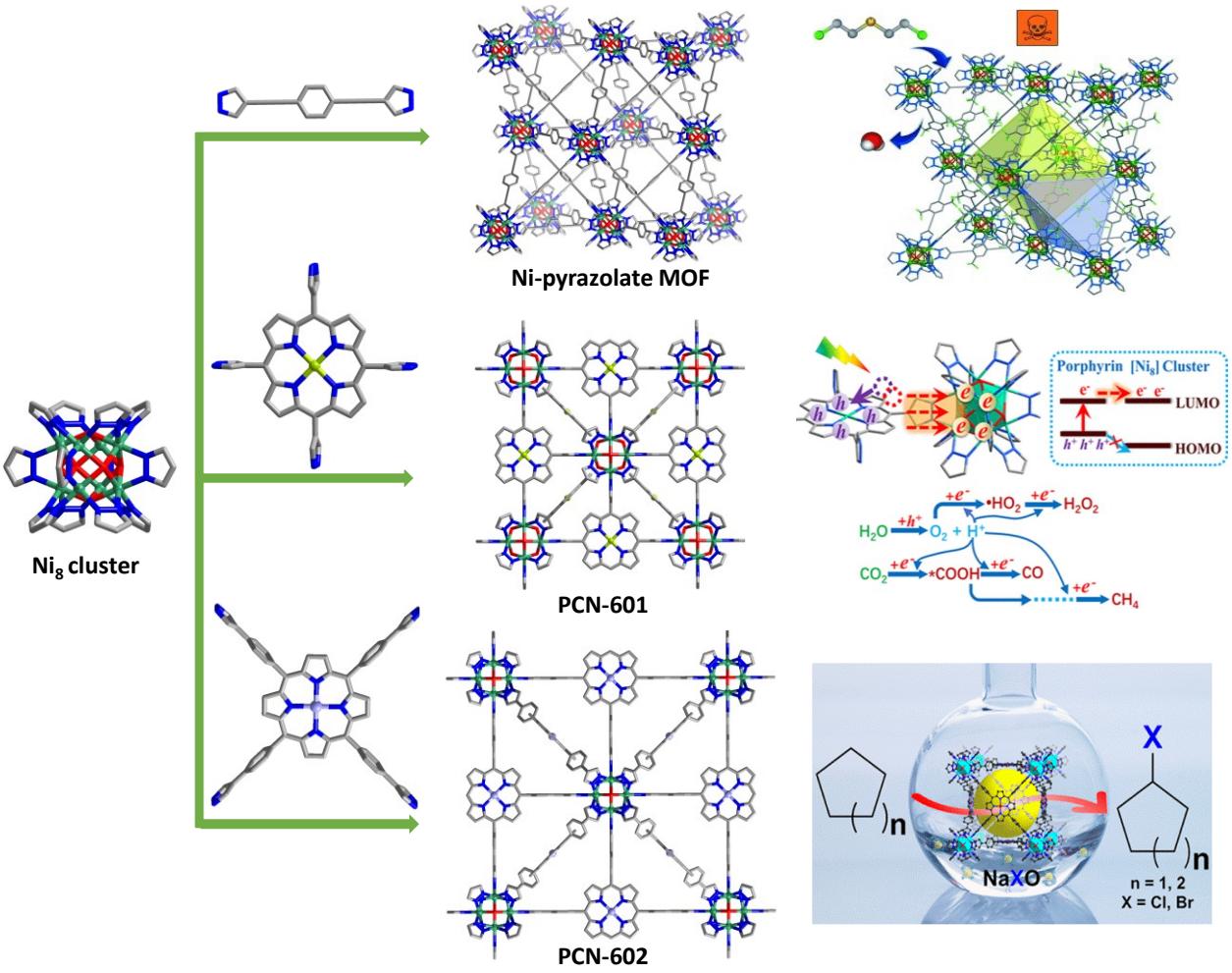

Fig. 6 The synthesis of metal-pyrazolate MOFs and their applications. Figure of the removal of volatile organic compound reprinted with permission from ref[42] (Copyright 2013 John Wiley and Sons); figure of the photoreduction of carbon dioxide to methane reprinted with permission from ref[78] (copyright 2020 The Royal Society of Chemistry); figure of the halogenation of C-H bonds in basic conditions reprinted with permission from ref[79] (Copyright 2017 American Chemical Society)

The 12-connected octanuclear nickel-containing cluster can geometrically be viewed as cuboctahedron, and the combination of this cuboctahedron and square building units results in the formation of MOFs based on the 4,12-connected **ftw** net. Li, Zhou, and coworkers synthesized a

stable porphyrinic Ni-MOF, denoted as PCN-601, from the assembly of 5,10,15,20-tetra(1*H*-pyrazol-4-yl)-porphyrin ligands and Ni_8 nodes.[77] PCN-601 shows excellent base resistance, as suggested by the maintenance of crystallinity and porosity after treatment with a saturated sodium hydroxide solution. A recent study revealed that PCN-601 can serve as an efficient catalyst for the photoreduction of carbon dioxide to methane.[78] The successful implementation of reticular chemistry allows the rational synthesis of the extended version of PCN-601, denoted as PCN-602, from the assembly of Ni_8 nodes and pyrazolate porphyrinic ligands with additional phenyl rings.[79] PCN-602 is base-resistant and an efficient, stable, and recyclable catalyst for the halogenation of C–H bonds in basic conditions.

Triazolate-based MOFs comprise another class of stable MOFs that are promising for many applications, including electrocatalysis, gas storage, and gas separation.[80, 81] For instance, MFU-4 which is assembled from Zn_5 nodes and bbta ligands (H_2bbta = 1*H*,5*H*-benzo(1,2-*d*:4,5-*d*′)bistriazole), is a robust cubic Zn-MOF with the **pcu** net.[82] Due to its small pore sizes, MFU-4 can be used for highly effective separation of a H_2/D_2 isotope mixture (**Fig. 7**).[83] The isoreticular expansion of MFU-4 through the use of the elongated linker H_2btdd (bis(1H-1,2,3-triazolo[4,5-b],[4′,5′-i])dibenzo[1,4]dioxin), results in the formation of the extended MOF MFU-4*l*.[84] Post-synthetical modification of MFU-4*l* enables the synthesis of a series of metalated MOFs, denoted as M-MFU-4*l*. Among them, Cu^{I}-MFU-4*l* shows promise as a hydrogen storage material due to the presence of its trigonal pyramidal open Cu^{+} sites that result in a H_2 isosteric heat of adsorption of about 32 kJ mol^{-1}.[85, 86] The post-synthetically exchanged MFU-4*l*-Li displays an impressive hydrogen deliverable capacity of 50.2 g L^{-1} and 9.4 wt% under the operating condition between 77 K / 100 bar and 160 K / 5 bar.[87] Finally, M-MFU-4*l* can be used as a catalyst for the hydrolytic

destruction of the nerve agent simulant dimethyl (4-nitrophenyl)phosphate, with tunable reactivity based on the identity of the metal incorporated into the node.[88]

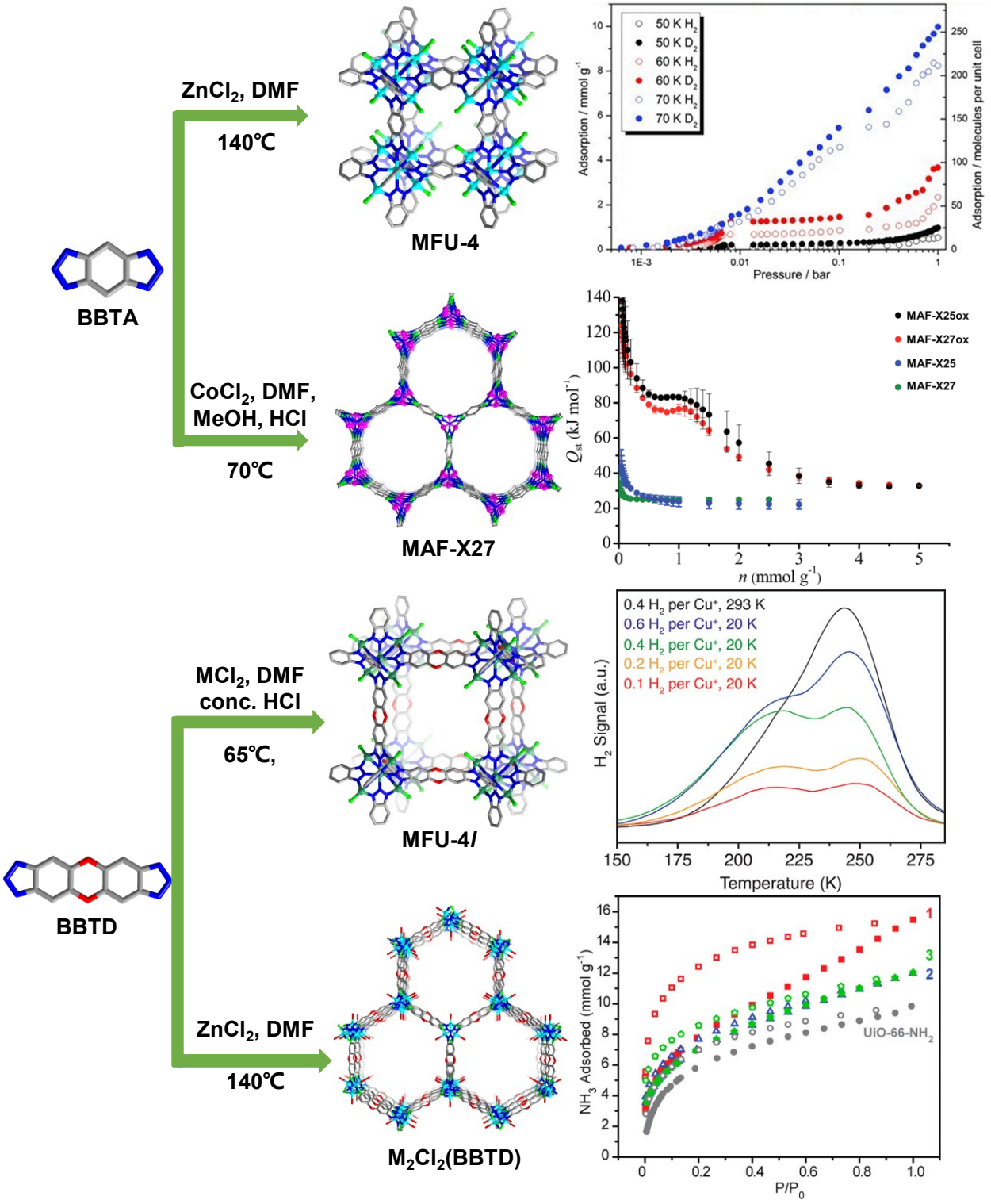

Fig. 7 The synthesis of triazolate-based MOFs and their applications. Gas adsorption and separation isotherms reprinted with permission from ref[83] (Copyright 2013 John Wiley and Sons), ref[81] (copyright 2015 The Royal Society of Chemistry), ref[86] (Copyright 2021 American Chemical Society), and ref[89] (Copyright 2016 American Chemical Society).

Zhang, Chen, and coworkers developed another important class of triazolate-based MOFs (e.g., MAF-X25[90] and MAF-X27[81]), which contain one type of hexagonal channel. MAF-X25 and MAF-X27, formulated as $[Mn^{II}_2Cl_2(bbta)]$ and $[Co^{II}_2Cl_2(bbta)]$, are synthesized from the assembly of H_2bbta and the metal salts $MnCl_2$ and $CoCl_2$, respectively, in the mixed solvents of DMF, methanol, and hydrochloric acid. MAF-X25 and MAF-X27 can further be treated with hydrogen peroxide to form $[Mn^{II}Mn^{III}(OH)Cl_2(bbta)]$ (MAF-X25ox) and $[Co^{II}Co^{III}(OH)Cl_2(bbta)]$ (MAF-X27ox), where monodentate hydroxide was introduced onto the oxidized metal sites.[81] Compared to the pristine MAF-X25 and MAF-X27 MOFs, MAF-X25ox and MAF-X27ox show significantly enhanced performance towards CO_2 capture, with CO_2 isosteric heats of adsorption of up to 124 kJ mol^{-1} and a CO_2 adsorption capacity of up to 9.1 mmol cm^{-3} at 298 K/1 bar. These MOFs display high chemical stability and gas adsorption-desorption recycling stability. Importantly, the MAF-X27 series retains its crystallinity even after treatment with a strong alkaline solution (1 M KOH) for 1 week, and they are efficient electrocatalysts for the oxygen evolution reaction.[80]

Dincă and coworkers synthesized a series of stable mesoporous triazolate-based MOFs, $M_2Cl_2(btdd)(H_2O)_2$ (M = Mn, Co, Ni), which are isoreticular to the MAF-X27 series, from the assembly of elongated linkers (H_2btdd) and related metal salts.[89] $M_2Cl_2(btdd)(H_2O)_2$ contain hexagonal pores of about 2.2 nm, as indicated by both SCXRD results and pore size distribution analysis. Due to their excellent stability under basic conditions, the $M_2Cl_2(btdd)$ series has been explored for ammonia capture, and the results from the sorption studies indicate that these MOFs

are stable after multiple ammonia adsorption-desorption cycles. Dincă and coworkers also investigated water sorption performance of M_2Cl_2(btdd) (M = Mn, Co, Ni).[21] Among these MOFs, Co_2Cl_2(btdd) is the best water adsorbent and displays a total water uptake of 0.968 g g^{-1} at the relative humidity of 94%.[21] Co_2Cl_2(btdd) is a promising adsorbent towards water sorption-related applications, such as atmospheric water generation and heat pumps.

Conclusion and Outlook

In this article, we provided an overview of the progress of the rational design and reticular synthesis of stable functional metal–organic framework (MOF) materials. One of the key advances in the MOF field resulted from the precise design of targeted, stable MOFs with controllable pore structures through the use of reticular chemistry approaches, which affords molecular-level control over pore sizes and pore geometries of the resulting MOFs. To fully transform structural functionalities of MOFs in macroscopic applications and enable the long-term and reliable use of MOFs, the stability of these materials is of great importance. For instance, depending on the functionalities explored and target environment for the application, chemical, hydrolytic, thermal, mechanical,[91] and radiation[92] stabilities of MOF materials can be crucial considerations. In this article, we covered two main types of stable MOFs that were guided by the HSAB principle, including high-valent metal-carboxylate MOFs and low-valent metal-azolate MOFs. Due to the limited length of this article, we primarily discussed the rational synthesis of chemically and hydrolytically stable MOFs and their applications in catalysis, water vapor capture, ammonia capture, gas separation, and storage.

Despite the tremendous progress in the past few years, plenty of room remains for the development of better synthetic strategies to generate stable functional MOFs that address current

challenges related to environmental and energy-related applications. We envision that advances in computational chemistry, including machine-learning and high-throughput screening, together with the automation chemistry system, could be a game-changer in creating a new generation of stable MOFs towards targeted applications. In addition, we encourage traditional chemists to explore diverse synthetic strategies (e.g., modulated synthesis and post-synthetic modification) with modern inorganic and organic chemistry to rationally design and synthesize complex MOF materials that remain relatively elusive, such as metal-phosphonate frameworks.

Acknowledgements

Z.C. gratefully acknowledges support by the National Natural Science Foundation of China (Grant No. 22201247) and the startup funding from Zhejiang University. O.K.F gratefully acknowledges support from the Army Research Office (W911NF2020136); the Defense Threat Reduction Agency (HDTRA1-22-1-0041); the Department of Energy (DE-SC0022332 and DE-FG02-08ER15967) and the National Science Foundation (CBET 2119433). K.O.K. gratefully acknowledges support from the IIN Postdoctoral Fellowship and the Northwestern University International Institute for Nanotechnology.

Competing interests

O.K.F. has a financial interest in NuMat Technologies, a startup company that is seeking to commercialize MOFs. All other authors declare no competing interests.

References

1 H. Furukawa, K. E. Cordova, M. O'Keeffe and O. M. Yaghi, *Science*, 2013, **341**, 1230444.

2 A. J. Howarth, Y. Liu, P. Li, Z. Li, T. C. Wang, J. T. Hupp and O. K. Farha, *Nat. Rev. Mater.*, 2016, **1**, 15018.

3 Y. Bai, Y. Dou, L.-H. Xie, W. Rutledge, J.-R. Li and H.-C. Zhou, *Chem. Soc. Rev.*, 2016, **45**, 2327-2367.
4 Z. Chen, M. C. Wasson, R. J. Drout, L. Robison, K. B. Idrees, J. G. Knapp, F. A. Son, X. Zhang, W. Hierse, C. Kühn, S. Marx, B. Hernandez and O. K. Farha, *Faraday Discuss.*, 2021, **225**, 9-69.
5 W. Gong, Z. Chen, J. Dong, Y. Liu and Y. Cui, *Chem. Rev.*, 2022, **122**, 9078-9144.
6 O. M. Yaghi, M. O'Keeffe, N. W. Ockwig, H. K. Chae, M. Eddaoudi and J. Kim, *Nature*, 2003, **423**, 705-714.
7 Z. Chen, H. Jiang, M. Li, M. O'Keeffe and M. Eddaoudi, *Chem. Rev.*, 2020, **120**, 8039-8065.
8 O. M. Yaghi, M. J. Kalmutzki and C. S. Diercks, *Introduction to Reticular Chemistry: Metal-Organic Frameworks and Covalent Organic Frameworks*, John Wiley & Sons, 2019.
9 H. Jiang, D. Alezi and M. Eddaoudi, *Nat. Rev. Mater.*, 2021, **6**, 466-487.
10 Z. Chen, Z. Thiam, A. Shkurenko, L. J. Weselinski, K. Adil, H. Jiang, D. Alezi, A. H. Assen, M. O'Keeffe and M. Eddaoudi, *J. Am. Chem. Soc.*, 2019, **141**, 20480-20489.
11 Z. Chen, Ł. J. Weseliński, K. Adil, Y. Belmabkhout, A. Shkurenko, H. Jiang, P. M. Bhatt, V. Guillerm, E. Dauzon, D.-X. Xue, M. O'Keeffe and M. Eddaoudi, *J. Am. Chem. Soc.*, 2017, **139**, 3265-3274.
12 Q. Liu, H. Cong and H. Deng, *J. Am. Chem. Soc.*, 2016, **138**, 13822-13825.
13 B. Tu, Q. Pang, D. Wu, Y. Song, L. Weng and Q. Li, *J. Am. Chem. Soc.*, 2014, **136**, 14465-14471.
14 B. Tu, Q. Pang, H. Xu, X. Li, Y. Wang, Z. Ma, L. Weng and Q. Li, *J. Am. Chem. Soc.*, 2017, **139**, 7998-8007.
15 Z. Chen, K. O. Kirlikovali, P. Li and O. K. Farha, *Acc. Chem. Res.*, 2022, **55**, 579-591.
16 Z. Chen, P. Li, R. Anderson, X. Wang, X. Zhang, L. Robison, L. R. Redfern, S. Moribe, T. Islamoglu, D. A. Gómez-Gualdrón, T. Yildirim, J. F. Stoddart and O. K. Farha, *Science*, 2020, **368**, 297-303.
17 N. Hanikel, M. S. Prévot and O. M. Yaghi, *Nat. Nanotechnol.*, 2020, **15**, 348-355.
18 T. Zhang and W. Lin, *Chem. Soc. Rev.*, 2014, **43**, 5982-5993.
19 M. Yoon, R. Srirambalaji and K. Kim, *Chem. Rev.*, 2012, **112**, 1196-1231.
20 W. Gong, X. Chen, H. Jiang, D. Chu, Y. Cui and Y. Liu, *J. Am. Chem. Soc.*, 2019, **141**, 7498-7508.
21 A. J. Rieth, S. Yang, E. N. Wang and M. Dincă, *ACS Cent. Sci.*, 2017, **3**, 668-672.
22 S. M. Towsif Abtab, D. Alezi, P. M. Bhatt, A. Shkurenko, Y. Belmabkhout, H. Aggarwal, Ł. J. Weseliński, N. Alsadun, U. Samin, M. N. Hedhili and M. Eddaoudi, *Chem*, 2018, **4**, 94-105.
23 Z. Chen, K. Ma, J. J. Mahle, H. Wang, Z. H. Syed, A. Atilgan, Y. Chen, J. H. Xin, T. Islamoglu, G. W. Peterson and O. K. Farha, *J. Am. Chem. Soc.*, 2019, **141**, 20016-20021.
24 K. O. Kirlikovali, Z. Chen, T. Islamoglu, J. T. Hupp and O. K. Farha, *ACS Appl. Mater. Interfaces*, 2020, **12**, 14702-14720.
25 J. M. Palomba, S. P. Harvey, M. Kalaj, B. R. Pimentel, J. B. DeCoste, G. W. Peterson and S. M. Cohen, *ACS Appl. Mater. Interfaces*, 2020, **12**, 14672-14677.
26 T. Islamoglu, Z. Chen, M. C. Wasson, C. T. Buru, K. O. Kirlikovali, U. Afrin, M. R. Mian and O. K. Farha, *Chem. Rev.*, 2020, **120**, 8130-8160.

27 D. Britt, D. Tranchemontagne and O. M. Yaghi, *Proc. Natl. Acad. Sci. U.S.A.*, 2008, **105**, 11623.
28 Z. Chen, K. O. Kirlikovali, K. B. Idrees, M. C. Wasson and O. K. Farha, *Chem*, 2022, **8**, 693-716.
29 K. Adil, Y. Belmabkhout, R. S. Pillai, A. Cadiau, P. M. Bhatt, A. H. Assen, G. Maurin and M. Eddaoudi, *Chem. Soc. Rev.*, 2017, **46**, 3402-3430.
30 X. Zhang, R.-B. Lin, J. Wang, B. Wang, B. Liang, T. Yildirim, J. Zhang, W. Zhou and B. Chen, *Adv. Mater.*, 2020, **32**, 1907995.
31 R.-B. Lin, L. Li, H.-L. Zhou, H. Wu, C. He, S. Li, R. Krishna, J. Li, W. Zhou and B. Chen, *Nat. Mater*, 2018, **17**, 1128-1133.
32 S. Yuan, L. Feng, K. Wang, J. Pang, M. Bosch, C. Lollar, Y. Sun, J. Qin, X. Yang, P. Zhang, Q. Wang, L. Zou, Y. Zhang, L. Zhang, Y. Fang, J. Li and H.-C. Zhou, *Adv. Mater.*, 2018, **30**, 1704303.
33 K. Wang, Y. Li, L.-H. Xie, X. Li and J.-R. Li, *Chem. Soc. Rev.*, 2022, **51**, 6417-6441.
34 T. Devic and C. Serre, *Chem. Soc. Rev.*, 2014, **43**, 6097-6115.
35 Q. Liu, Y. Song, Y. Ma, Y. Zhou, H. Cong, C. Wang, J. Wu, G. Hu, M. O'Keeffe and H. Deng, *J. Am. Chem. Soc.*, 2019, **141**, 488-496.
36 J.-P. Zhang, Y.-B. Zhang, J.-B. Lin and X.-M. Chen, *Chem. Rev.*, 2012, **112**, 1001-1033.
37 F. Yang, G. Xu, Y. Dou, B. Wang, H. Zhang, H. Wu, W. Zhou, J.-R. Li and B. Chen, *Nat. Energy*, 2017, **2**, 877-883.
38 M. Ding, X. Cai and H.-L. Jiang, *Chem. Sci.*, 2019, **10**, 10209-10230.
39 M. Eddaoudi, J. Kim, N. Rosi, D. Vodak, J. Wachter, M. O'Keeffe and O. M. Yaghi, *Science*, 2002, **295**, 469-472.
40 J. F. Eubank, F. Nouar, R. Luebke, A. J. Cairns, Ł. Wojtas, M. Alkordi, T. Bousquet, M. R. Hight, J. Eckert, J. P. Embs, P. A. Georgiev and M. Eddaoudi, *Angew. Chem. Int. Ed.*, 2012, **51**, 10099-10103.
41 Z. Chen, S. L. Hanna, L. R. Redfern, D. Alezi, T. Islamoglu and O. K. Farha, *Coord. Chem. Rev.*, 2019, **386**, 32-49.
42 N. M. Padial, E. Quartapelle Procopio, C. Montoro, E. López, J. E. Oltra, V. Colombo, A. Maspero, N. Masciocchi, S. Galli, I. Senkovska, S. Kaskel, E. Barea and J. A. R. Navarro, *Angew. Chem. Int. Ed.*, 2013, **52**, 8290-8294.
43 D. Zhang, Y. Zhu, L. Liu, X. Ying, C.-E. Hsiung, R. Sougrat, K. Li and Y. Han, *Science*, 2018, **359**, 675.
44 L. Liu, Z. Chen, J. Wang, D. Zhang, Y. Zhu, S. Ling, K.-W. Huang, Y. Belmabkhout, K. Adil, Y. Zhang, B. Slater, M. Eddaoudi and Y. Han, *Nat. Chem.*, 2019, **11**, 622-628.
45 A. Schaate, P. Roy, A. Godt, J. Lippke, F. Waltz, M. Wiebcke and P. Behrens, *Chem. Eur. J.*, 2011, **17**, 6643-6651.
46 A. C. Sudik, A. P. Côté and O. M. Yaghi, *Inorg. Chem.*, 2005, **44**, 2998-3000.
47 C. Serre, C. Mellot-Draznieks, S. Surblé, N. Audebrand, Y. Filinchuk and G. Férey, *Science*, 2007, **315**, 1828.
48 Y. K. Hwang, D.-Y. Hong, J.-S. Chang, H. Seo, M. Yoon, J. Kim, S. H. Jhung, C. Serre and G. Férey, *Appl. Catal., A.*, 2009, **358**, 249-253.
49 J. Kim, S. Bhattacharjee, K.-E. Jeong, S.-Y. Jeong and W.-S. Ahn, *Chem. Commun.*, 2009, 3904-3906.

50 J. W. Yoon, H. Chang, S.-J. Lee, Y. K. Hwang, D.-Y. Hong, S.-K. Lee, J. S. Lee, S. Jang, T.-U. Yoon, K. Kwac, Y. Jung, R. S. Pillai, F. Faucher, A. Vimont, M. Daturi, G. Férey, C. Serre, G. Maurin, Y.-S. Bae and J.-S. Chang, *Nat. Mater*, 2017, **16**, 526.
51 T.-F. Liu, L. Zou, D. Feng, Y.-P. Chen, S. Fordham, X. Wang, Y. Liu and H.-C. Zhou, *J. Am. Chem. Soc.*, 2014, **136**, 7813-7816.
52 X. Lian, D. Feng, Y.-P. Chen, T.-F. Liu, X. Wang and H.-C. Zhou, *Chem. Sci.*, 2015, **6**, 7044-7048.
53 Y. Liu, J. F. Eubank, A. J. Cairns, J. Eckert, V. C. Kravtsov, R. Luebke and M. Eddaoudi, *Angew. Chem. Int. Ed.*, 2007, **46**, 3278-3283.
54 M. Pang, A. J. Cairns, Y. Liu, Y. Belmabkhout, H. C. Zeng and M. Eddaoudi, *J. Am. Chem. Soc.*, 2013, **135**, 10234-10237.
55 Y. Belmabkhout, R. S. Pillai, D. Alezi, O. Shekhah, P. M. Bhatt, Z. Chen, K. Adil, S. Vaesen, G. De Weireld, M. Pang, M. Suetin, A. J. Cairns, V. Solovyeva, A. Shkurenko, O. El Tall, G. Maurin and M. Eddaoudi, *J. Mater. Chem. A*, 2017, **5**, 3293-3303.
56 H. Chevreau, A. Permyakova, F. Nouar, P. Fabry, C. Livage, F. Ragon, A. Garcia-Marquez, T. Devic, N. Steunou, C. Serre and P. Horcajada, *CrystEngComm*, 2016, **18**, 4094-4101.
57 A. Dhakshinamoorthy, M. Alvaro, H. Chevreau, P. Horcajada, T. Devic, C. Serre and H. Garcia, *Catal. Sci. Technol.*, 2012, **2**, 324-330.
58 D. Feng, K. Wang, Z. Wei, Y.-P. Chen, C. M. Simon, R. K. Arvapally, R. L. Martin, M. Bosch, T.-F. Liu, S. Fordham, D. Yuan, M. A. Omary, M. Haranczyk, B. Smit and H.-C. Zhou, *Nat. Commun.*, 2014, **5**, 5723.
59 H. F. Drake, G. S. Day, S. W. Vali, Z. Xiao, S. Banerjee, J. Li, E. A. Joseph, J. E. Kuszynski, Z. T. Perry, A. Kirchon, O. K. Ozdemir, P. A. Lindahl and H.-C. Zhou, *Chem. Commun.*, 2019, **55**, 12769-12772.
60 Z. Chen, X. Wang, R. Cao, K. B. Idrees, X. Liu, M. C. Wasson and O. K. Farha, *ACS Materials Lett.*, 2020, **2**, 1129-1134.
61 D. Alezi, Y. Belmabkhout, M. Suyetin, P. M. Bhatt, Ł. J. Weseliński, V. Solovyeva, K. Adil, I. Spanopoulos, P. N. Trikalitis, A.-H. Emwas and M. Eddaoudi, *J. Am. Chem. Soc.*, 2015, **137**, 13308-13318.
62 Z. Chen, P. Li, X. Zhang, P. Li, M. C. Wasson, T. Islamoglu, J. F. Stoddart and O. K. Farha, *J. Am. Chem. Soc.*, 2019, **141**, 2900-2905.
63 J. Zhu, P.-Z. Li, W. Guo, Y. Zhao and R. Zou, *Coord. Chem. Rev.*, 2018, **359**, 80-101.
64 H. Assi, G. Mouchaham, N. Steunou, T. Devic and C. Serre, *Chem. Soc. Rev.*, 2017, **46**, 3431-3452.
65 M. Dan-Hardi, C. Serre, T. Frot, L. Rozes, G. Maurin, C. Sanchez and G. Ferey, *J. Am. Chem. Soc.*, 2009, **131**, 10857-10859.
66 Y. Fu, D. Sun, Y. Chen, R. Huang, Z. Ding, X. Fu and Z. Li, *Angew. Chem. Int. Ed.*, 2012, **51**, 3364-3367.
67 B. Bueken, F. Vermoortele, D. E. P. Vanpoucke, H. Reinsch, C.-C. Tsou, P. Valvekens, T. De Baerdemaeker, R. Ameloot, C. E. A. Kirschhock, V. Van Speybroeck, J. M. Mayer and D. De Vos, *Angew. Chem. Int. Ed.*, 2015, **54**, 13912-13917.
68 S. Yuan, T.-F. Liu, D. Feng, J. Tian, K. Wang, J. Qin, Q. Zhang, Y.-P. Chen, M. Bosch, L. Zou, S. J. Teat, S. J. Dalgarno and H.-C. Zhou, *Chem. Sci.*, 2015, **6**, 3926-3930.
69 L. Zou, D. Feng, T.-F. Liu, Y.-P. Chen, S. Yuan, K. Wang, X. Wang, S. Fordham and H.-C. Zhou, *Chem. Sci.*, 2016, **7**, 1063-1069.

70 Y.-H. Xiao, P. Weidler, S.-S. Lin, C. Wöll, Z.-G. Gu and J. Zhang, *Adv. Funct. Mater*, 2022, **32**, 2204289.
71 W. Gong, H. Xie, K. B. Idrees, F. A. Son, Z. Chen, F. Sha, Y. Liu, Y. Cui and O. K. Farha, *J. Am. Chem. Soc.*, 2022, **144**, 1826-1834.
72 W. Gong, Y. Xie, X. Wang, K. O. Kirlikovali, K. B. Idrees, F. Sha, H. Xie, Y. Liu, B. Chen, Y. Cui and O. K. Farha, *J. Am. Chem. Soc.*, 2023, **145**, 2679-2689.
73 Y. Chen, K. B. Idrees, M. R. Mian, F. A. Son, C. Zhang, X. Wang and O. K. Farha, *J. Am. Chem. Soc.*, 2023, **145**, 3055-3063.
74 X.-C. Huang, Y.-Y. Lin, J.-P. Zhang and X.-M. Chen, *Angew. Chem. Int. Ed.*, 2006, **45**, 1557-1559.
75 K. S. Park, Z. Ni, A. P. Côté, J. Y. Choi, R. Huang, F. J. Uribe-Romo, H. K. Chae, M. O'Keeffe and O. M. Yaghi, *Proc. Natl. Acad. Sci. U.S.A.*, 2006, **103**, 10186-10191.
76 N. Masciocchi, S. Galli, V. Colombo, A. Maspero, G. Palmisano, B. Seyyedi, C. Lamberti and S. Bordiga, *J. Am. Chem. Soc.*, 2010, **132**, 7902-7904.
77 K. Wang, X.-L. Lv, D. Feng, J. Li, S. Chen, J. Sun, L. Song, Y. Xie, J.-R. Li and H.-C. Zhou, *J. Am. Chem. Soc.*, 2016, **138**, 914-919.
78 Z.-B. Fang, T.-T. Liu, J. Liu, S. Jin, X.-P. Wu, X.-Q. Gong, K. Wang, Q. Yin, T.-F. Liu, R. Cao and H.-C. Zhou, *J. Am. Chem. Soc.*, 2020, **142**, 12515-12523.
79 X.-L. Lv, K. Wang, B. Wang, J. Su, X. Zou, Y. Xie, J.-R. Li and H.-C. Zhou, *J. Am. Chem. Soc.*, 2017, **139**, 211-217.
80 X.-F. Lu, P.-Q. Liao, J.-W. Wang, J.-X. Wu, X.-W. Chen, C.-T. He, J.-P. Zhang, G.-R. Li and X.-M. Chen, *J. Am. Chem. Soc.*, 2016, **138**, 8336-8339.
81 P.-Q. Liao, H. Chen, D.-D. Zhou, S.-Y. Liu, C.-T. He, Z. Rui, H. Ji, J.-P. Zhang and X.-M. Chen, *Energy Environ. Sci.*, 2015, **8**, 1011-1016.
82 S. Biswas, M. Grzywa, H. P. Nayek, S. Dehnen, I. Senkovska, S. Kaskel and D. Volkmer, *Dalton Trans.*, 2009, 6487-6495.
83 J. Teufel, H. Oh, M. Hirscher, M. Wahiduzzaman, L. Zhechkov, A. Kuc, T. Heine, D. Denysenko and D. Volkmer, *Adv. Mater.*, 2013, **25**, 635-639.
84 D. Denysenko, M. Grzywa, M. Tonigold, B. Streppel, I. Krkljus, M. Hirscher, E. Mugnaioli, U. Kolb, J. Hanss and D. Volkmer, *Chem. Eur. J.*, 2011, **17**, 1837-1848.
85 D. Denysenko, M. Grzywa, J. Jelic, K. Reuter and D. Volkmer, *Angew. Chem. Int. Ed.*, 2014, **53**, 5832-5836.
86 B. R. Barnett, H. A. Evans, G. M. Su, H. Z. H. Jiang, R. Chakraborty, D. Banyeretse, T. J. Hartman, M. B. Martinez, B. A. Trump, J. D. Tarver, M. N. Dods, L. M. Funke, J. Börgel, J. A. Reimer, W. S. Drisdell, K. E. Hurst, T. Gennett, S. A. FitzGerald, C. M. Brown, M. Head-Gordon and J. R. Long, *J. Am. Chem. Soc.*, 2021, **143**, 14884-14894.
87 Z. Chen, M. R. Mian, S.-J. Lee, H. Chen, X. Zhang, K. O. Kirlikovali, S. Shulda, P. Melix, A. S. Rosen, P. A. Parilla, T. Gennett, R. Q. Snurr, T. Islamoglu, T. Yildirim and O. K. Farha, *J. Am. Chem. Soc.*, 2021, **143**, 18838-18843.
88 M. R. Mian, H. Chen, R. Cao, K. O. Kirlikovali, R. Q. Snurr, T. Islamoglu and O. K. Farha, *J. Am. Chem. Soc.*, 2021, **143**, 9893-9900.
89 A. J. Rieth, Y. Tulchinsky and M. Dincă, *J. Am. Chem. Soc.*, 2016, **138**, 9401-9404.
90 P.-Q. Liao, X.-Y. Li, J. Bai, C.-T. He, D.-D. Zhou, W.-X. Zhang, J.-P. Zhang and X.-M. Chen, *Chem. Eur. J.*, 2014, **20**, 11303-11307.

91 L. Robison, R. J. Drout, L. R. Redfern, F. A. Son, M. C. Wasson, S. Goswami, Z. Chen, A. Olszewski, K. B. Idrees, T. Islamoglu and O. K. Farha, *Chem. Mater.*, 2020, **32**, 3545-3552.

92 C. Volkringer, C. Falaise, P. Devaux, R. Giovine, V. Stevenson, F. Pourpoint, O. Lafon, M. Osmond, C. Jeanjacques, B. Marcillaud, J. C. Sabroux and T. Loiseau, *Chem. Commun.*, 2016, **52**, 12502-12505.

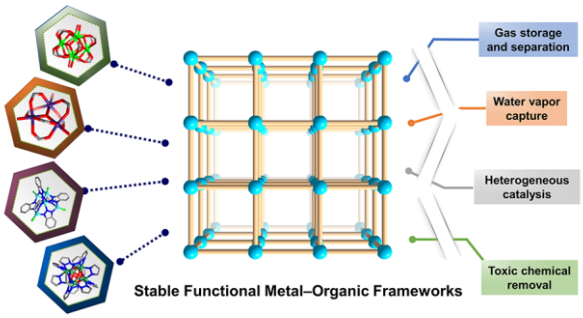

We reviewed the rational design and synthesis of stable metal–organic frameworks (MOFs) with controllable pores and functionalities. The implementation of reticular chemistry allows the synthesis of stable MOFs with targeted topological nets and programmable pores, for diverse applications ranging from water vapor capture, catalysis, toxic chemical removal, to gas storage and separation.